Materials and Structures/Matériaux et Constructions, Vol. **36**, March 2003, pp 118-126

The effect of reinforcement in the new layer on hygral cracking in hybrid structural elements

O. Bernard [1,2] and E. Brühwiler [3]

(1) Department of Civil and Environmental Engineering, Massachusetts Institute of Technology, Cambridge, USA

(2) OXAND, Ingénierie et Technologie, Montigny-sur-Loing, France

(3) Department of Civil Engineering, Swiss Federal Institute of Technology, Lausanne, Switzerland

Paper received: May 3, 2001; Paper accepted: November 23, 2001

ABSTRACT

In structural elements consisting of concretes of different ages (hybrid elements), hygral deformations induced by drying of the new concrete are restrained by the old concrete. Depending on the amplitude of these deformations and on the degree of restraint of the hybrid element, cracks can be induced in the new concrete layer. An experimental investigation conducted during six months on twelve hybrid elements demonstrated that global displacements are reduced when the reinforcement ratio placed in the new layer is increased. Comparison of the experimental results with a numerical model shows that the presence of reinforcement in the new layer increases the degree of restraint of hygral deformations and the likelihood of localized cracks.

RÉSUMÉ

Dans les éléments de structure formés de bétons d'âges différents (éléments hybrides), les déformations induites par le séchage de la nouvelle couche sont entravées par le support de vieux béton. En fonction de l'amplitude de ces déformations et du degré d'entrave de la structure hybride, des fissures peuvent être induites dans la nouvelle couche. Des essais de fluage flexionnel réalisés durant six mois sur douze éléments de structure hybride ont permis de mettre en évidence que leurs déplacements induits par le séchage de la nouvelle couche sont réduits lorsque le taux d'armature placé dans cette couche augmente. En s'appuyant sur les résultats obtenus lors de la validation de la modélisation numérique proposée, cet article démontre que la présence de barres d'armature dans la nouvelle couche augmente l'entrave de ses déformations de séchage et favorise l'apparition de fissures.

1. INTRODUCTION

Casting a new concrete layer on an existing support is a common technique in the repair and strengthening of existing reinforced concrete structures. During the hydration of the new concrete, physical and chemical deformations induced by heat release and autogenous shrinkage are totally or partially restrained by the presence of the old concrete layer. The old concrete also restrains deformations caused by the drying of the new concrete after removal of the formwork (see Fig. 1). Depending on the magnitude of these deformations and the degree of restraint of the hybrid element, detrimental cracks can be induced in the new concrete layer at an early age or after a longer period of time [1]. If these cracks reach the interface between the two concretes debonding may occur (see Fig. 1).

This paper explains the findings of a research project investigating the long term behaviour of structural elements consisting of concretes of different ages, herein called hybrid elements. Concentration is on the effect of reinforcement on the cracking due to drying (herein

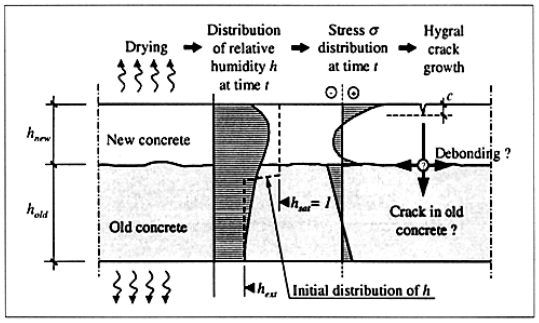

Fig. 1 – Influence of drying on hybrid elements.

Editorial Note

Prof. Eugen Brühwiler is a RILEM Senior Member. He works at EPFL, a RILEM Titular Member and participates as a corresponding member in RILEM TC 189-NEC 'Non-destructive evaluation of the "covercrete" (concrete cover)'.

called hygral cracking) of the new concrete layer in hybrid elements. Their behaviour is studied using both experimental and numerical methods.

2. RELATED WORKS

Most research on the behaviour of hybrid elements has been conducted in the past two decades. The main contributions are related to the study of the long-term behaviour of layers of new concrete subjected to drying (see [2-4] for layers thinner than 60 mm and [5, 6] for thicker layers). These studies have established that the penetration of cracks in the new concrete layer depends mainly on two categories of parameters: 1) *material properties*, such as the magnitude of drying shrinkage, the ratio between tensile specific creep and drying shrinkage and the tensile strength of the new concrete, and the ratio between tensile elastic modulus of new and old concretes; and 2) *structural parameters*, such as the thickness of new concrete layer, the ratio between the thickness of new and old concrete layers and the degree of statical indetermination which depends on the static system of the hybrid structure.

A simplified approach to estimate the stresses in the new layer of hybrid elements consists in multiplying the degree of restraint μ by the product of free physical and chemical deformations ε_k and elastic modulus E_{new} of the new concrete layer. Silfwerbrand [7] established an expression of μ for statically determinant hybrid slabs by assuming time-independent elastic behaviour of concrete and constant deformation ε_k in the new concrete. This expression has been generalized for various types of hybrid structures and for statically indeterminate systems in [5]. The assumption of constant deformation ε_k in the new concrete is only a rough approximation of the real distribution of deformations or relative humidity due to drying $\varepsilon_{k,sh}$. Due to the low diffusion coefficient of concrete, a sharp moisture gradient occurs between the core and the surface zone of the new concrete layer to balance the external conditions of relative humidity [8]. Depending on the concrete composition and the thickness of a structural element, the magnitude of the moisture gradient can be high enough to induce microcracking in the surface zone even if the structural element is not externally restrained [9] (the core of the element restrains the drying shrinkage of the surface zone).

The reinforcement, which is not affected by drying, is generally located near the surface zone. It has been demonstrated that this reinforcement modifies the distribution of microcracking in the surface zone [10, 11]. The reinforcement increases the degree of restraint of drying deformations.

As the moisture transport in the cement paste is a slow process, the time required to reach moisture equilibrium in a concrete structural element depends on the thickness of the elements. For example, Acker [8] estimated that this equilibrium is reached after ten years in a cylinder of 160 mm diameter subjected to a external relative humidity of 50%. It has also been shown that the total tensile creep of new concrete plays an important role in releasing the internal stresses created by the non-uniform distribution of moisture and restraint imposed by the old concrete [5]. For hybrid elements with high degree of restraint, it has been established in [5] that the beneficial effect of tensile creep can limit the hygral cracking and prevent the formation of full-depth crack and thus also prevent debonding. These results were confirmed in [6] using a micromechanical model of concrete. This study also illustrated the beneficial influence on cracking of aggregates in the new concrete. Laurence [12] demonstrated that the hygral cracking observed on the surface of new layers thinner than 60 mm does not depend significantly on the tensile relaxation of concrete. Ulm *et al.* [10] also demonstrated that the microcracking of the surface zone is not significantly influenced by the relaxation of concrete. These results can be explained by the high and rapidly forming initial gradients of moisture, which cause this microcracking in the surface zone. The time to cracking is too short to have a beneficial effect of tensile relaxation.

3. EXPERIMENTAL STUDY

3.1 Tested hybrid elements

Twelve hybrid beams were fabricated and tested (see Fig. 2). The supports were cast with a length/width/thickness of 5400/500/170 mm. At the age of 60 days, the upper surface of the supports was prepared with a hydrojetting technique to reduce the thickness by 20 mm. Two weeks later, the interface was cleaned and moistened with water for one hour. At 70 days, the new concrete layer was cast on the support. The two vertical faces and the bottom part of the hybrid elements were sealed with an epoxy coating to avoid drying after 100 days (see Fig. 3). The tested elements were kept in a controlled environment (T_{ext} = 20 ± 3°C and h_{ext} = 65 ± 5%) before the beginning of the testing procedure.

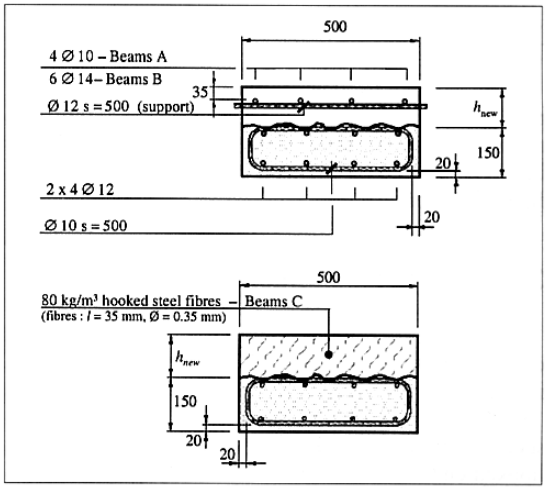

Fig. 2 – Cross sections of tested beams.

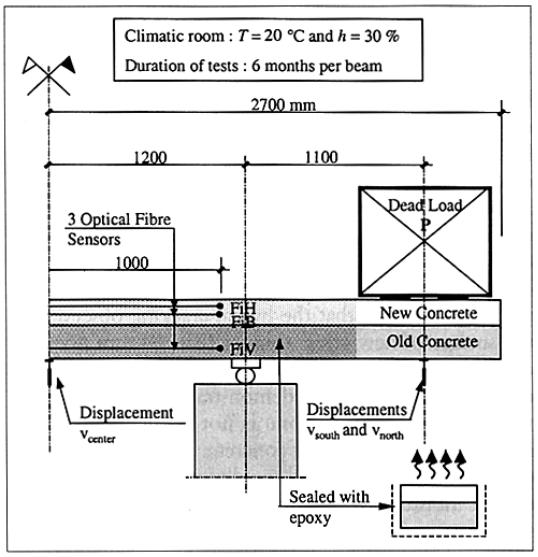

Fig. 3 – Boundary conditions and instrumentation.

Table 1 – Parameters of tested beams				
Beams	h_{new} [mm]	Reinfor. in new layer	Dead Load P [kg]	Age t_0 [days]
A1	70	4 ϕ 10	880	178
A2	120	4 ϕ 10	1200	178
A3	120	4 ϕ 10	1510	178
A4	120	4 ϕ 10	0	178
B1	70	6 ϕ 14	880	178
B2	120	6 ϕ 14	1200	404
B3	120	6 ϕ 14	0	404
B4	120	6 ϕ 14	1510	404
C1	70	Fiber	880	466
C2	120	Fiber	0	466
C3	120	Fiber	1510	466
C4	120	Fiber	1510	466

The variable parameters illustrated in Table 1 were the thickness of the new layer h_{new} (70 and 120 mm) and the reinforcement type of the new layer (4 Ø 10 for beams A, 6 Ø 14 for beams B or only 80 kg/m^3 of steel fibers for beams C).

3.2 Concrete compositions

The concrete compositions in this investigation used ordinary Portland cement CEM I 52,5 R and are given in Table 2. The cement was composed of 54.5% of C_3S, 15.9% of C_2S, 8.1% of C_3A and 7.6% C_4AF and the specific surface was 4300 cm^2/g (Blaine finesse). The hooked ends steel fibers were 35 mm long with diameters of 350 µm.

Table 2 – Concrete compositions			
	Old Concrete All beams [kg/m^3]	New Concrete	
		beams A+B [kg/m^3]	beams C [kg/m^3]
Agg. *8 - 16 mm*	640	612	580
Agg. *4 - 8 mm*	588	644	588
Sand *0 - 4 mm*	715	687	715
Steel fibres	-	-	80
Cement CEM I 52.5 R	350	300	350
Total water	161	150	171
w/c [-]	0.46	0.50	0.49
Rheobuild 2000†	3.50	3.60	3.50

† *Rheobuild 2000 is a superplasticiser from Master Builders Technologies.*

3.3 Testing procedure and instrumentation

3.3.1 Long term flexural tests on hybrid elements

Each beam was placed in a climatic room (T_{ext} = 20 ± 3°C and h_{ext} = 30 ± 5%) three days prior to testing (the age t_0 of the new concrete prior to testing is given in Table 1). The static system used during the tests and the position of dead loads imposed at time t_0 are described in Fig. 3. The imposed values of P are given in Table 1. The load level was selected to be representative of the permanent serviceability loading of hybrid elements. The loads placed on beams A1, A2, A3 and B1 were introduced in two stages (80% of P at time t_0 and 20% after 14 days). The beams A4, B3 and C2 were not loaded during the tests. The tests conducted on loaded beams will be called herein flexural creep tests on hybrid elements (FCTHE) and those conducted without dead loads are called flexural shrinkage tests on hybrid elements (FSTHE). Each beam was tested for a 6-month period.

Three vertical displacements (v_{north}, v_{center} and v_{south}) were measured during the flexural tests. The vertical displacements due to the imposed loads are assumed to be positive. The location of the displacement transducers is shown in Fig. 3. Each beam was instrumented with 3 optical fibre sensors [13] during casting. The 3-level position of these sensors is shown in Fig. 3 (FiV for bottom of the support, FiB and FiH for bottom and top of the new layer). The optical fiber sensors measured total displacements at the beam mid-span (distance 2000 mm). The evolution of cracking in the new concrete was observed visually on the upper and vertical surfaces of the hybrid elements.

3.3.2 Flexural shrinkage tests without old concrete layer (FSTWO)

Flexural shrinkage tests were carried out independently to study the influence of reinforcement on the vertical displacements due to drying of a non-restrained concrete element. Four beams were cast with a length/width/thickness of 1150/100/100 mm. A reinforcing bar (diameter 10 mm) was placed in the bottom of two of the beams (concrete cover 20 mm). The concrete composition was similar to that used for the new concrete layer of beams A

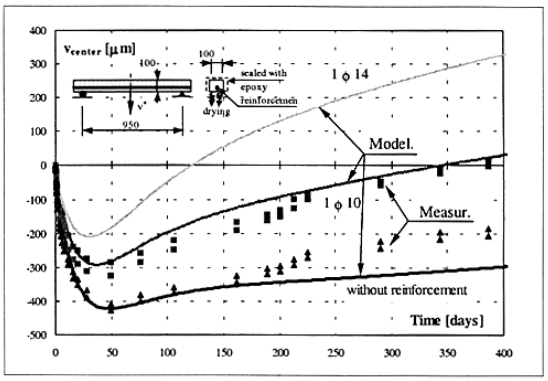

Fig. 4 – Experimental and numerical results related to the flexural shrinkage test without old concrete layer (FSTWO): influence of reinforcement.

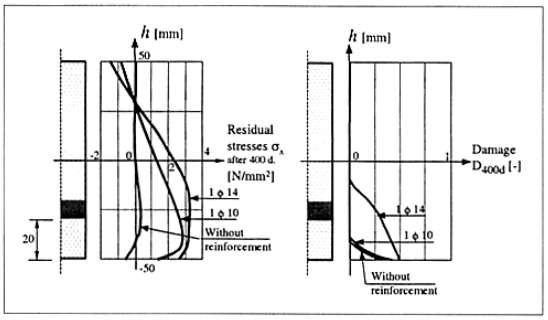

Fig. 5 – Numerical calculation of residual stresses and damage in the FSTWO beams: influence of reinforcement.

and B (see Table 2) however the cement type, CEM I 42.5, was coarser. During the first day, the tested beams were kept in the steel formwork. They were then placed in water for 5 days. At 6 days, the tested beams were removed from the water and the sides and the top of each beam were sealed with an epoxy coating (see Fig. 4). At 7 days, the four tested beams were placed in a climatic room (T_{ext} = 20 ± 3°C and h_{ext} = 30 ± 5%). The static system used during the tests is shown in Fig. 4. The vertical displacement of each beam was measured during the testing procedure (see Fig. 4). The duration of these flexural shrinkage tests without old concrete layer (FSTWO) was 1 year.

3.4 Experimental results

3.4.1 Flexural shrinkage tests without old concrete layer (FSTWO)

The evolution of the vertical displacements of the four beams is shown in Fig. 4. During the first 50 days, the central part of each beam rose due to drying (negative vertical displacement according to the chosen convention). The results show that the presence of reinforcement reduces this displacement. As the reinforcement restrains the hygral deformations in the bottom of the beam, the observed reduction of vertical displacement is an expected result. After 50 days, the direction of the displacements is reversed. For a purely elastic material, the beam would return to its initial shape after drying. For the tested beams without reinforcement, a residual displacement was still measured after 1 year. This residual displacement was probably due to the non-completed reclosure of the hygral cracks in the surface zone. After 350 days, the vertical displacement of reinforced beams became positive. This result can be explained by the effect of creep due to the dead weight of the beam. No visible cracking was observed on the bottom of the beams during the tests.

3.4.2 Flexural shrinkage tests on hybrid elements (FSTHE)

The evolution of vertical displacements of beams A4, B3 and C2 are illustrated in Figs. 6 a), b) and c) respectively. The ends (v_{north} and v_{south}) of beam A4 rose almost linearly due to drying (negative vertical displacement according to the chosen convention) and the center (v_{center}) went down. This behaviour of beam A4 was almost as expected. The behaviour of beam B3 however was significantly different. The vertical displacements remained small. The differences between beams A4 and B3 were the reinforcement ratio placed in the new layer (4 O 10 for A4 and 6 O 14 for B3) and the age of the new concrete at the beginning of the test (t_0 = 178 days for A4 and 404 days for B3).

It is believed that this difference was predominately due to the reinforcement ratio as the observed behaviour of beam C2, with a new concrete of 466 days at t_0, was very close to that of the beam A4. It is important to recall that the new concrete of beam C2 is a non-reinforced steel fibre concrete. The increased reinforcement restrained more severely the hygral deformations in the surface zone and thus reduced the vertical displacements of the hybrid elements. The different values of time t_0 had a negligible influence on the tests.

The evolution of total strains at the mid-span of beam A4, measured with the optical fibre sensors, are shown in Fig. 7 a). The time and the measured strains in Fig. 7 a) are assumed to be 0 at the age t_0 of the beam. The total strains for the negative values of time are due to the thermal and autogenous effects at early age and drying. The early age behaviour of the tested elements is studied in [5]. It is interesting to notice that the magnitude of the early age strains is near 300 µm/m and that the magnitude of strains measured during the FSTHE is only 50 µm/m.

3.4.3 Flexural creep tests on hybrid elements (FCTHE)

The evolution of the total strains at mid-span of beam A2, measured with the optical fibre sensors, is shown in Fig. 7 b). The observed behaviour is similar to that observed on the non-loaded beam A4 (see Fig. 7 a). Again, it is interesting to notice that the magnitude of mechanical strains due to loading is approximately seven times lower than the amplitude of strains due to hydration effects at early age and drying.

The evolution of total vertical displacements of beams A1 and B1 (h_{new} = 70 mm) and of beams A2 and

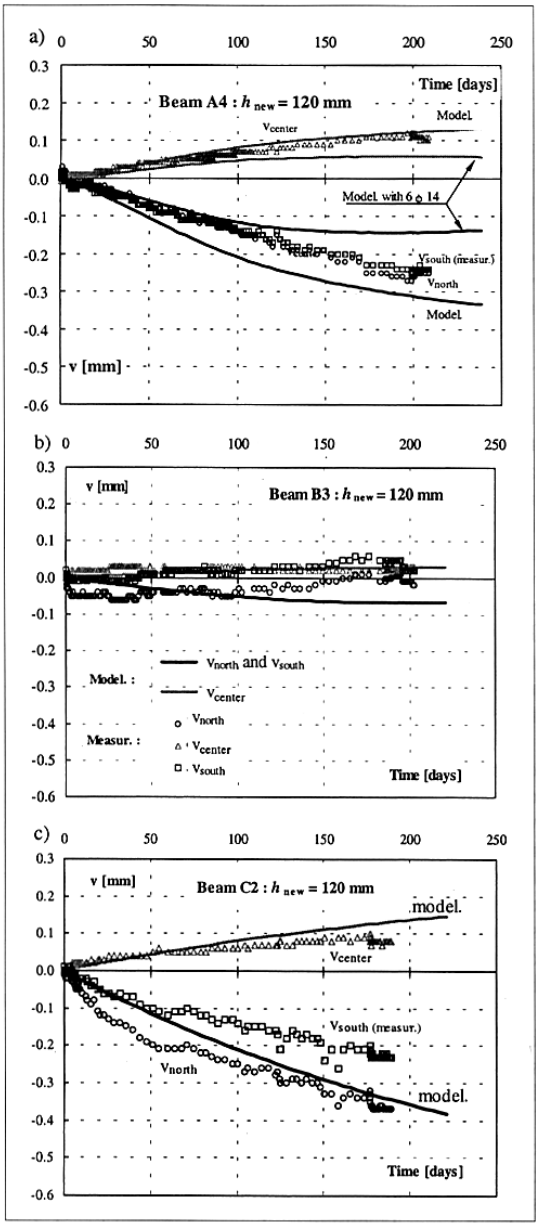

Fig. 6 – Experimental and numerical evolution of displacements of beams a) A4, b) B3 and c) C2 during the flexural shrinkage test on hybrid elements (FSTHE).

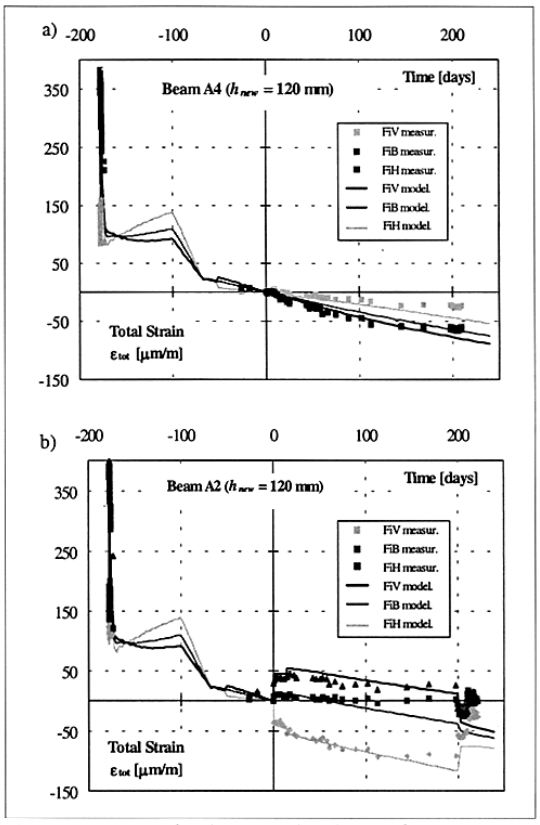

Fig. 7 – Experimental and numerical evolution of total strains in the center of the beams a) A4 during the FSTHE and b) A2 during the flexural creep tests on hybrid elements (FCTHE).

B2 are shown in Fig. 8 a), b) and 11 a), b), respectively. Comparison of these figures shows that the elastic instantaneous displacements of beams A1 and B1 are similar. The time-dependent displacements of beam B1 are however greater than those of beam A1. Similar results can be observed on beams A2 and B2. The higher reinforcement ratio in the new concrete increased the amplitude of total vertical displacements measured with time. An initial explanation is that the higher reinforcement ratio increases the effect of creep. It should be kept in mind that the measured displacements correspond to the summation of positive displacements due to creep and negative displacements due to drying shrinkage. As observed in the FSTHE, the displacements due to drying shrinkage decrease with the increase in reinforcement ratio. If we assume that the principle of superposition is applicable, the higher total displacements observed on beams B1 and B2 can be explained with the reduction of negative hygral displacements due to the higher reinforcement ratio in the new layers.

The behaviour of beams C was similar to that observed on beams A. The displacements measured on all beams are given in [14].

The beam B1 was the only beam, which exhibited localized vertical cracks in the new layer during the FCTHE. The cracked zone near the north support is shown in Fig. 9. No visible cracks were found during the preliminary check of the surfaces of new concrete layer done before the FCTHE. It can therefore be assumed that the observed cracks appeared during the FCTHE. The new layer of concrete in beam B1 was thin and had a high reinforcement ratio. Beam A1, which was similar to B1, except for a lower reinforcement ratio, exhibited no visible cracks. This result confirms the influence of reinforcement on the increase in degree of restraint of

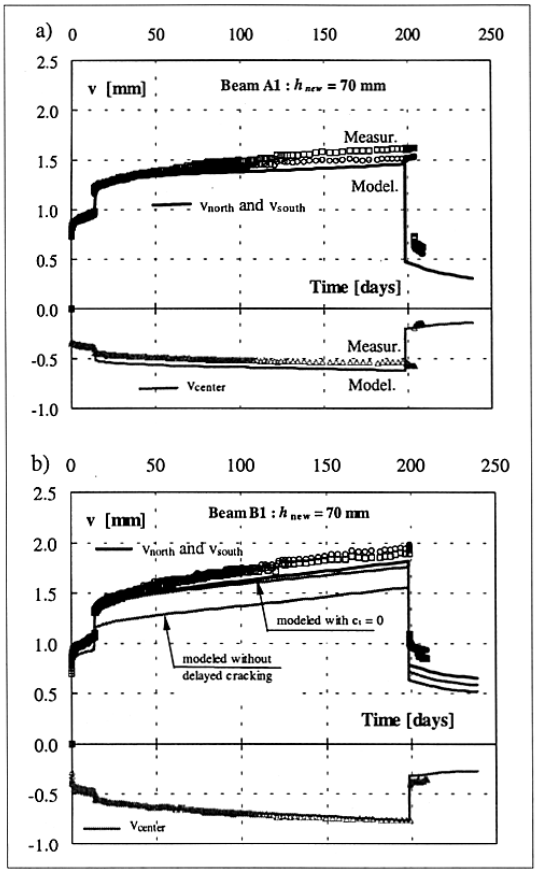

Fig. 8 – Experimental and numerical evolution of displacements of beams a) A1 and b) B1 during the flexural creep test on hybrid elements (FCTHE).

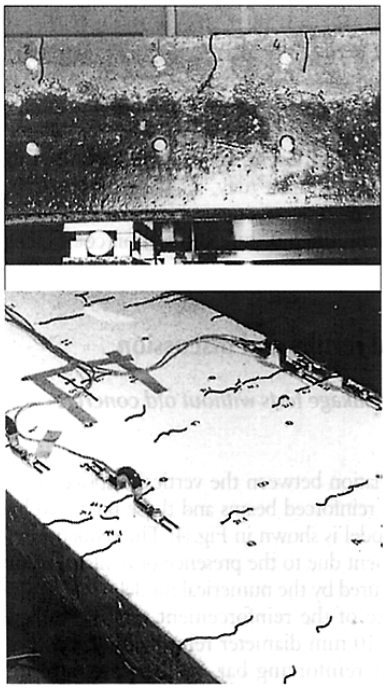

Fig. 9 – Cracking of the new concrete of beam B1 during the FCTHE.

hygral deformations in the new layer and on the increase in likelihood of cracking.

4. NUMERICAL STUDY

The previous experimental results have revealed that the presence of reinforcement in the new layer enhances the restraint of hygral deformations. Internal stresses are promoted and hygral cracking seems to be more pronounced. As these new findings are of great interest with regard to the durability of repaired concrete elements, it appears essential to analyze them by means of a numerical approach. The following study demonstrates the capabilities of the numerical model to reproduce the observed behaviour. The focus of the simulation also is to determine the amplitude of internal stresses and the cracking due to the presence of reinforcement in the new layer of hybrid structural elements.

4.1 Description of modelling

The long-term behaviour of hybrid elements subjected to drying was modelled using the Finite Element software *HEAT* 6.3 (developed by Femmasse b.v. Company). This software was developed by Roelfstra [9]. Recent modifications have been made to improve the models of the hygral- and time-dependent cracking behaviour of concrete [5].

The analysis consisted in solving a boundary value problem (BVP) for relative humidity as well as stresses. The formulation of the BVP for *relative humidity* was based on the Bažant model [15] and is given by:

$$\dot{h} = \operatorname{div}\left(D(h)\,\operatorname{grad} h\right) + \dot{h}_{hydr} \qquad (1)$$

$$\text{with } D(h) = D_0\left[a_h + \frac{1-a_h}{1+\left(\frac{1-h}{1-h_c}\right)^4}\right]$$

$$q = \pi\left(h - h_{ext}\right) n \quad \text{(on the boundary)} \qquad (2)$$

where h: relative humidity of concrete, h_{hydr}: decrease in relative humidity due to hydration, $D(h)$: diffusion coefficient ($D_0 = D(h = 1)$), q: moisture flux through the surface, π: moisture convection coefficient, h_{ext}: external relative humidity, n: outward unit normal to surface and a_h, h_c are parameters.

After computation of the relative humidity distribution, a *stress analysis* was carried out. The formulation of the BVP for stresses is given by:

$$\dot{\sigma} = S_{ve}\left(\dot{\varepsilon}_{total} - \dot{\varepsilon}_k\right) \qquad (3)$$

$$T = \bar{T} \quad \text{and} \quad u = \bar{u} \quad \text{(on the boundary)} \qquad (4)$$

where $T = \sigma \cdot n$: stress vector acting on the surface, σ: stress

tensor, S_{ve}: viscoelasticity tensor, ε_{total}: total strain tensor, ε_k: tensor of the physical strains due to drying calculated with a constant coefficient of hygral dilation α_h, $\overline{T}$: imposed stress vector and $\overline{u}$: prescribed displacements.

The *viscoelastic behaviour* was modeled with a generalized Maxwell model [16]:

$$\sigma_n = \sum_{\mu=1}^{6} \Delta\sigma_n^{\mu} + \sum_{\mu=1}^{6} \sigma_{n-1}^{\mu} e^{-\frac{\Delta t}{\tau_\mu}} \qquad (5)$$

$$\text{with} \quad \Delta\sigma_n^{\mu} = \left[\frac{\tau_\mu}{\Delta t} E_\mu \left(1 - e^{-\frac{\Delta t}{\tau_\mu}} \right) \right] A \left[\Delta\varepsilon_{total} - \Delta\varepsilon_k \right]$$

where μ = 1 to 6 Maxwell unit number with E_μ: spring modulus, τ_μ: dashpot retardation time, σ_n: stress tensor at time t_n, $\Delta t = t_n - t_{n-1}$: time increment and A: tensor containing the terms related to the Poisson ratio ν.

The *non-linear influence of relative humidity and tensile stress level on the stress rate* was taken into account with the time equivalent method [15, 17]. Δt is corrected with:

$$\Delta t_{corr} = \left(a_t - (1 - a_t) h^2 \right) \left(\frac{\sinh\left(c_t \frac{\sigma_1}{f_{ct}} \right)}{c_t \frac{\sigma_1}{f_{ct}}} \right) \Delta t \qquad (6)$$

where σ_1: major principal stress, f_{ct}: tensile strength of concrete and a_t, c_t are parameters. The *hygral transient creep* (Pickett effect) was taken into account by introducing a stress-dependent contribution [18] in the coefficient of hygral dilation ($\alpha_{h,\sigma} = \alpha_h - r_\sigma \sigma_1$) where r_σ: parameter.

The *cracking behaviour* of concrete was modelled with strain-softening smeared-type model [19]. A bilinear relationship (σ, w) depending on the fictitious crack width w ($\sigma = f_{ct}$, $w = 0$; αf_c, w_1; 0, w_c) was used after the principal tensile stress reached the tensile strength f_{ct}. In this crack model, the damage (denoted D in Figs. 5 and 10) corresponds to the ratio between the effective stiffness of a cracked and uncracked concrete element. For example, only non-localized microcracks (fictitious crack width less than 10 µm) can be expected for a value of D less than 0.50. In order to model the failure of concrete under sustained or repeated load, the tensile strength f_{ct} was modelled as a function of the pure viscous total strain ε_{vis} [5] (a_{cr} b_{cr} c_{cr}: parameters):

$$\frac{f_{ct}(\varepsilon_{vis})}{f_{ct}} = 1 - \left(a_{cr} \left(1 - e^{-b_{cr} \varepsilon_{vis}} \right) \right)^{c_{cr}} \qquad (7)$$

The *reinforcement* was modelled with beam-type finite elements superimposed on membrane-type finite elements used to represent the concrete. The compatibility between these two types of finite elements is regulated with a typical steel-concrete adherence law ($\tau = as^b$ with τ: shear stress, s: slip, a and b parameters) [20]. More details concerning the modelling can be found in [5].

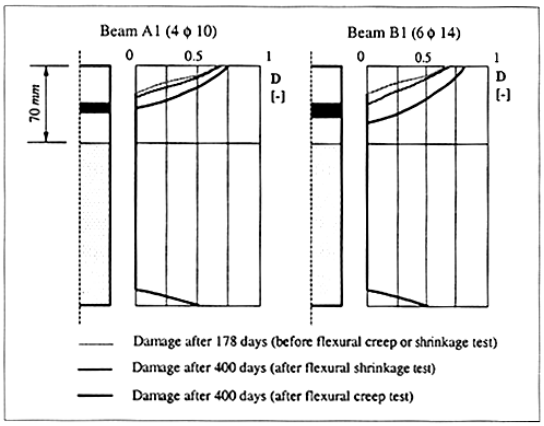

Fig. 10 – Damage calculated in beams A1 and B1.

4.2 Determination of parameters

The parameters were determined by means of results obtained with standard tests [14], which were totally independent of the experimental results presented in this paper. When standard tests were not conducted, values available in the literature (see references in [5]) were used to determine the corresponding parameters. As the drying process of concrete could not be separated from the total viscoelastic behaviour, an iterative procedure was developed to determine the required parameters (see details in [5]). For the concretes described in Table 2, the obtained parameters are: D_0 = 50 mm²/day, a_h = 0.05, h_c = 0.82, h_{hydr} = 0, $\alpha_{h,old}$ = 1000 µm/m, $\alpha_{h,new}$ = 1715 µm/m (final shrinkage $\varepsilon_{cs,\infty}$ = 600 µm/m for h_{ext} = 0.65), $f_{ct,new}$ = 3.7 MPa, $f_{ct,old}$ = 4.4 MPa, $f_{ct,interface}$ = 2.8 MPa, $E_{new} = E_{int}$ = 37.0 GPa, E_{old} = 44.5 GPa, ν = 0.16, $\tau_\mu = 10^{(\mu-1)}$ with μ = 1 to 6, E_1/E_{tot} = 0.02, E_2/E_{tot} = 0.04, E_3/E_{tot} = 0.07, E_4/E_{tot} = 0.14, E_5/E_{tot} = 0.27, E_6/E_{tot} = 0.46, a_t = 0.5, c_t = 3.8, r_σ = 5 MPa^{-1}, α = 0.25, w_1 = 0.03 mm, w_c = 0.30 mm, a_{cr} = 0.3, b_{cr} = 50, c_{cr} = 0.25, a = 12.3 and b = 0.21. The elastic modulus of reinforcement was 210 GPa. Due to the different cement type, the following parameters were different for the concrete used in the FSTWO: D_0 = 36 mm²/day, a_h = 0.10, h_c = 0.70, $\alpha_{h,old}$ = 1200 µm/m. For a concrete surface in a non-windy environment, the moisture convection coefficient π is equal to 1 mm/day.

4.3 Numerical results and discussion

4.3.1 Flexural shrinkage tests without old concrete layer (FSTWO)

A good correlation between the vertical displacements measured on the reinforced beams and those predicted by the numerical model is shown in Fig. 4. The reduction of vertical displacement due to the presence of reinforcement is rather well captured by the numerical model.

The influence of the reinforcement ratio is studied by replacing the 10 mm diameter reinforcing bar with a 14 mm diameter reinforcing bar. In this case, a more

pronounced reduction of the vertical displacement is predicted by the numerical model. Residual stresses calculated after 400 days are shown in Fig. 5. For the non-reinforced beams, the residual stresses are not significant. For the reinforced beams, tensile stresses were present in a large portion of the beam. As the equilibrium must maintained, compressive stresses act in the reinforcement. As the magnitude of residual stresses is directly related to the restraint due to the reinforcement, the tensile residual stresses increase when the reinforcement ratio increases. The microcracked zone for different reinforcement ratios is also shown in Fig. 5. The damage predicted after 400 days is similar for the two types of beam used in the experimental study. For these beams, the microcracked zone did not extend to the reinforcement. For beams with a 14 mm reinforcing bar, the microcracked zone was shown to pass the level of reinforcement. Even though the damage D remains smaller than 0.50 (no visible cracks), the protection of reinforcement against corrosion is questionable in this last case.

4.3.2 Flexural shrinkage tests on hybrid elements (FSTHE)

A comparison between the calculated vertical displacements of beams A4, B3 and C2 and the corresponding measured values can be seen in Figs. 6 a), b) and c). The smaller vertical displacements of beam B3 are accurately reproduced by the numerical model. There is also a good correlation between the predicted and measured strains at both early age and long term at the mid-span of beam A4 (Fig. 7 a)). As the accuracy of the numerical model has been verified using two independent measuring techniques, it is demonstrated that this model can be used to reproduce the behaviour of reinforced hybrid elements subjected to drying.

Fig. 6 a) shows the calculated vertical displacements for a hypothetical beam similar to A4 but reinforced with 6 Ø 14 instead of 4 Ø 10. Again, the presence of a higher reinforcement ratio explains the lower magnitude of the observed vertical displacements due to drying. The results show that the real behaviour of beams acting before the age t_0 at the beginning of the flexural tests must be considered in order to obtain accurate predictions with the model.

4.3.3 Flexural creep tests on hybrid elements (FCTHE)

The influence of the superimposed dead load is also well captured by the numerical model (see the measured and predicted strains in the central part of the beam A2 at both early age and long term in Fig. 7 b) and the calculated and measured vertical displacements for beams A1 and B1, and A2 and B2 in Figs. 8 a), b) and 11 a), b), respectively).

The evolution of vertical displacements of beam A2 were calculated without taking into account the influence of tensile stress level on the stress rate (c_t = 0 in Equation (6)) and without delayed cracking due to sustained load (a_{cr} = 0 in Equation (7) (Fig. 8 b)). The numerical results show that the influence of the tensile stress level is not significant. On the contrary, the influence of sustained load on the reduction of tensile strength must be taken into account in order to predict accurate vertical displacements.

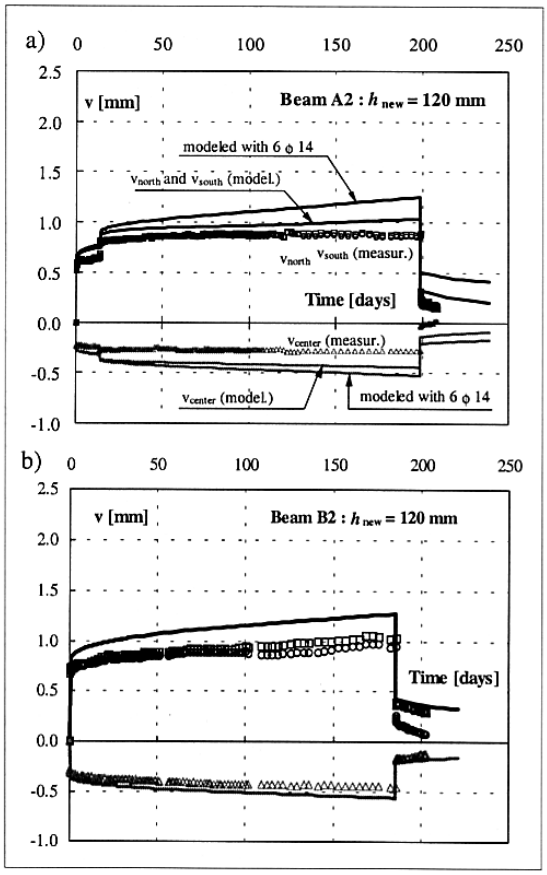

Fig. 11 – Experimental and numerical evolution of displacements of beams a) A2 and b) B2 during the FCTHE.

Fig. 11 a) shows the calculated vertical displacements for a hypothetical beam similar to A2 but reinforced with 6 Ø 14 instead of 4 Ø 10. Again, the presence of a higher reinforcement ratio explains the higher amplitude of observed vertical displacements.

By separating the two contributions of the calculated vertical displacements it can be seen that since the vertical displacements due to creep alone are similar for beams A1 and B1, the observed difference between total vertical displacements is predominantly due to the influence of the reinforcement ratio on the vertical displacement due to drying.

The damage calculated in beams A1 and B1 is shown in Fig. 10. The more pronounced damage observed in beam B1 was predicted by the numerical model. The calculated depth of the microcracked zone corresponds well with experimental observations (Fig. 9). The different causes of damage are stated in Fig. 10. The majority of the damage is due to the drying process alone. Even if the imposed loads were similar for beams A1 and B1, the additional damage would be more pronounced in beam B1 due to the higher residual stresses caused by drying in

the more reinforced beam B1. This important result demonstrates clearly that the presence of a large amount of reinforcement can enhance the extent of the microcracking in the new layer of hybrid elements.

5. CONCLUSIONS

The following conclusions about the behaviour of structural elements consisting of reinforced concretes of different ages subjected to drying are based on the experimental and numerical results reported in this paper:
1) Reinforcement in the new layer of concrete increases locally the degree of restraint of hygral deformations;
2) Due to the increased restraint of the hygral deformations by the reinforcement the global displacements of the hybrid structural element are reduced and more pronounced hygral cracking is induced in the new layer;
3) Residual tensile stresses due to drying are present in the long term in the new layer. The magnitude of these stresses depends predominantly on the reinforcement ratio;
4) When a service load is superimposed on an hybrid element subjected to drying, the mechanical stresses are added to the residual stresses due to drying and cracking can be more pronounced;
5) Irrespective of the degree of restraint, the depth of the hygral microcracked zone of a concrete element with a high reinforcement ratio can be larger than the thickness of the covercrete and can thus reach the level of reinforcement.

A minimal reinforcement ratio is usually required by the codes in order to control the cracking in concrete structures. Based on our results, it seems also important to limit the maximum amount of reinforcement in order to reduce the extent of the hygral microcracked zone. Even if the relationship between the depth of microcracked zone and the corrosion protection of the reinforcement is not the scope of this paper, it seems obvious that limiting the extend of microcracking in general will improve the durability of concrete structures. For the hybrid structural elements, such new criterion should define the maximum amount of reinforcement as a function of the thickness of the new layer.

REFERENCES

[1] Krauss, P. D. and Rogalla, E. A., 'Transverse cracking in newly constructed bridge decks', NCHRP Report 380, Transportation Research Board, National Research Council, (1996).

[2] Bissonnette, B., 'Le fluage en traction: un aspect important de la problématique des réparations minces en béton', Doctoral thesis of Laval University, Quebec City, Canada, (1996).

[3] Martinola, G. and Wittmann, F. H., 'Application of fracture mechanics to optimize repair mortar systems', in 'Fracture Mechanics of Concrete Structures', Proceedings of FRAMCOS-2, F. H.Wittmann Ed., Aedificatio, (1995), 1481-1492.

[4] Sadouki, H. and van Mier, J. G. M., 'Simulation of hygral crack growth in concrete repair systems', *Mater. Struct.* **30** (1997) 518-526.

[5] Bernard, O., 'Comportement à long terme des éléments de structure formés de bétons d'âges différents', Doctoral thesis, Swiss Federal Institute of Technology n° 2283, Lausanne, Switzerland, (2000).

[6] Cécot, C., 'Étude micromécanique par simulation numérique en éléments finis des couplages viscoélasticité-croissance des fissures dans les composites granulaires de type béton', Doctoral thesis, Swiss Federal Institute of Technolgy n° 2365, Lausanne, Switzerland, (2001).

[7] Silfwerbrand, J., 'Stresses and strains in composite concrete beams subjected to differential shrinkage', *ACI Structural Journal* **94** (4) (1997), 347-353.

[8] Acker, P., 'Comportement mécanique du béton: apports de l'approche physico-chimique', LPC Reseach Report n° 152, LCPC, Paris, France, (1988).

[9] Roelfstra, P., 'A numerical approach to investigate the properties of concrete - numerical concrete', Doctoral thesis, Swiss Federal Institute of Technology n° 788, Lausanne, Switzerland, (1989).

[10] Ulm, F.-J., Schaller, I., Chauvel, D., Rossi, P. and De Larrard, F., 'Minimum reinforcement in nuclear cooling towers: FE-durability analysis of concrete cracking due to drying', in 'Utilization of High Strength / High Performance Concrete', Fourth International Symposium BHP96, Paris, France, (1996), 1163-1173.

[11] Nmai, C. K., Tomita, R., Hondo, F. and Buffenbarger, J., 'Shrinkage reducing admixtures', *Concrete International* **20** (4) (1998), 31-37.

[12] Laurence, O., 'La fissuration due au retrait restreint dans les réparations minces en béton: apports combinés de l'expérimentation et de la modélisation', Doctoral thesis of Laval University and ENPC, Quebec City, Canada, Paris, France (2001).

[13] Inaudi, D., 'Fiber optic sensor network for the monitoring of civil engineering structures', Doctoral thesis, Swiss Federal Institute of Technology n° 1612, Lausanne, Switzerland, (1997).

[14] Bernard, O., 'Comportement à long terme des éléments de structure formés de bétons d'âges différents', Test report n° 96.01.01, (2000).

[15] Bažant, Z. P. and Najjar, L. J., 'Nonlinear water diffusion in non saturated concrete', *Mater. Struct.* **5** (1985), 1-20.

[16] Bažant, Z. P. and Wu, S. T., 'Rate-type creep law of aging concrete based on Maxwell chain', *Mater. Struct.* **17** (37) (1974), 45-52.

[17] Eyring, H., 'Viscosity, plasticity and diffusion as examples of absolute reaction rates', *Journal of Chem. Phys.* **14** (1936), 283-291.

[18] Bažant, Z. P. and Chern, J. C., 'Concrete creep at variable humidity: constitutive law and mechanism', *Mater. Struct.* **18** (103) (1985), 1-20.

[19] Bažant, Z. P. and Oh, B.H., 'Crack band theory for fracture of concrete', *Mater. Struct.* **16** (1983), 155-177.

[20] Mivelaz, P., 'Étanchéité des structures en béton armé: fuites au travers d'un élément fissuré', Doctoral thesis, Swiss Federal Institute of Technology n° 1539, Lausanne, Switzerland, (1996).